Materials Research Bulletin 187 (2025) 113380

Contents lists available at ScienceDirect

Materials Research Bulletin

journal homepage: www.elsevier.com/locate/matresbu

Research Papers

Microstructure and properties of thin AlN coatings with different stoichiometric compositions

Vasilina Lapitskaya [a,*], Andrey Nikolaev [b], Anastasiya Khabarava [a], Evgeniy Sadyrin [b], Sergei Aizikovich [b], Aleksandr Komarov [c], Dmitry Orda [c], Aleksandra Cherniavskaya [c], Kamaludin Abdulvakhidov [d], Anaid Azoyan [e], Dmitry Kotov [f], Sergei Chizhik [a]

[a] Nanoprocesses and Technology Laboratory, A.V. Luikov Heat and Mass Transfer Institute of the National Academy of Science of Belarus, 15 P. Brovki Str., 220072 Minsk, Belarus
[b] Research and Education Center "Materials", Don State Technical University, 1 Gagarin Sq., 344000 Rostov-on-Don, , Russia
[c] Laboratory of Modification Technologies of Engeneering Materials, Joint Institute of Mechanical Engineering of the National Academy of Sciences of Belarus, 12 Akademicheskaya Str., 220012 Minsk, Republic of Belarus
[d] Southern Federal University, Sladkova 178/24, 344090 Rostov-on-Don, Russia
[e] Rostov State Transport University, 2 Rostovskogo Strelkovogo Polka Narodnogo Opolcheniya Sq., 344038 Rostov-on-Don, Russia
[f] Academic department of Micro- and Nanoelectronics, Belarusian State University of Informatics and Radioelectronics, P. Browka 6, 220013 Minsk, Belarus

ARTICLE INFO

Keywords:
Aln coating
Magnetron sputtering
Microstructure
Mechanical and microtribological properties
Specific electrical resistivity

ABSTRACT

The influence of the stoichiometric composition of thin AlN coatings on its microstructure, properties and specific electrical resistivity was studied. It was established that a sharp change occurs in the microstructure and properties when the nitrogen concentration in the coatings varies from 15 to 20 at.% N due to the changes in the phase composition of coatings. High mechanical properties (elastic modulus E and microhardness H) were obtained on $Al_{0.87}N_{0.13}$ coating (E = 65 GPa, H = 1.1 GPa, group 1, at sputtering temperature 100 °C) and $Al_{0.86}N_{0.14}$ coating (E = 65 GPa, H = 1.2 GPa, group 2, at sputtering temperature 20 °C). Low microtribological properties were obtained: in group 1 on an $Al_{0.87}N_{0.13}$ coating and in group 2 – $Al_{0.83}N_{0.17}$ coating. From the point of view of the optimal combination of microstructure and properties the most preferred AlN coatings for use in microelectronics are: from group 1 – $Al_{0.87}N_{0.13}$ coating (ρ=0.168 μΩ·m), from group 2 – $Al_{0.83}N_{0.17}$ coating (ρ=0.918 μΩ·m).

1. Introduction

Aluminum nitride (AlN) coatings demonstrate excellent piezoelectric properties [1,2], wide bandgap [3], low coefficient of thermal expansion, high thermal conductivity [4–6], resistivity and dielectric properties [4]. Due to these properties, they are widely used in electronic [1] and optoelectronic [3,5,7] equipment. As a good piezoelectric material [8,9] AlN is utilized in surface acoustic wave devices [2,10,11]. In microelectronics such a material can be combined with silicon technologies [2]. Due to the wide bandgap (6.2 eV) AlN coatings have found wide application in optoelectronic devices in the UV range [3,5]. AlN coatings are also used as wear-resistant and impact-resistant coatings with dielectric properties for elements of electronic equipment [12]. AlN coatings can be used as intermediate layers [13] with variable hardness to create a hybrid coating on which a diamond-like coating (DLC) is deposited, which makes it possible to reduce the distribution of mechanical stress in the DLC and increase the adhesive strength [13].

AlN application in multilayer coatings with alternating CrN and AlN layers of various thicknesses [14,15] makes it possible to create a gradient in the atomic and electronic structures due to the presence of phase transformations and, thus to improve the complex of properties for the resulting material. Multilayer AlN/Al coatings (the individual layers of which effectively crystallize tend) deposited by magnetron sputtering method to be dense and smooth and are used as corrosion-resistant and scratch-resistant coatings to protect various surfaces [16]. Nanometer-scale individual layers in AlN/Al multilayer coatings with different thicknesses of an individual AlN layer can significantly change the mechanical, tribological and optical properties of the surface [17,18]. Ni-doped AlN coatings exhibit excellent ferromagnetic properties [19].

* Corresponding author at: Minsk, 220072, P. Brovki Str. 15, Belarus.
E-mail address: vasilinka.92@mail.ru (V. Lapitskaya).

https://doi.org/10.1016/j.materresbull.2025.113380
Received 22 March 2024; Received in revised form 11 January 2025; Accepted 17 February 2025
Available online 18 February 2025

Table 1
AlN coating deposition parameters.

Group	Sample №	N_2 flow [sccm]	Power [W]	Temperature [°C]
1	1.1	1	150	100
	1.2	2		
	1.3	3		
	1.4	4		
	1.5	5		
2	2.1	0.75	100	20
	2.2	1.50		
	2.3	2.25		
	2.4	3.00		
	2.5	3.75		

Table 2
Thickness and stoichiometric composition of AlN coatings.

Sample №	Thickness [nm]	at. % N	at. % Al
1.1	833±42	6.31±0.24	93.69±0.24
1.2	789±39	12.98±0.32	87.02±0.32
1.3	725±36	19.46±0.77	80.54±0.77
1.4	875±44	25.48±0.70	74.52±0.70
1.5	1220±61	32.55±0.12	67.45±0.12
2.1	950±48	5.88±0.46	94.12±0.46
2.2	876±44	14.47±0.47	85.53±0.47
2.3	800±40	19.04±0.53	80.96±0.53
2.4	1050±53	17.16±0.47	82.84±0.47
2.5	1000±50	26.69±0.19	73.31±0.19

Practical tasks in the fields of microelectronics, design of communication devices and optoelectronic equipment require high quality of the transmitted signal, for which achievement structure, color and surface roughness of the coatings plays a crucial role [2,10,11,20–22].

There are various methods for deposition of AlN coatings: chemical vapor deposition, molecular beam epitaxy, reactive plasma spraying, excimer laser synthesis, magnetron sputtering process, plasma-enhanced atomic layer deposition [2,3,14,23–26]. However, the problem of reproducibility of the structure, required properties and stoichiometric composition when depositing coatings, as well as degradation and fracture of the coatings subjected to high temperatures used in most coating deposition methods still remains [5].

To expand the possibility of using AlN coatings in microdevices, it is necessary to comprehensively characterize the properties of coatings in microcontacts. For such purposes, probe research methods are used – atomic force microscopy (to study the microstructure) and nanoindentation (to determine mechanical and microtribological properties).

The purpose of this work is to study the influence of the stoichiometric composition of AlN coatings deposited by the magnetron sputtering method on their microstructure, mechanical, tribological properties and specific electrical resistivity.

2. Materials and methods

AlN coatings were obtained by reactive DC magnetron sputtering of Al using the VSM 100 (ROBVAC, Russia) magnetron system on silicon substrates of (100) orientation at a constant pressure of 0.78 Pa in the closed chamber of the system [27]. The samples were sputtered in the power stabilization mode, which was 100 and 150 W at temperatures of 20 and 100 °C (Table 1). The nitrogen flow varied for the first group from 1 to 5 sccm with a step of 1 sccm, and for the second group – from 0.75 to 3.75 sccm with a step of 0.75 sccm (Table 1). Sputtering was carried out at a constant rotation speed of the samples. Before each sputtering, the target was cleaned by sputtering in an inert Ar atmosphere for 15 mins at a sputtering power of 100 W. After deposition, the coated samples were cleaved along a previously applied notch on the back side of the Si substrate. The thickness of the coatings was further determined using a Crossbeam 340 scanning electron microscope (SEM, Carl Zeiss Micrography, Germany). During the study, the samples were fixed in a special holder so that the surface of the cross-section was located normally under the electron beam. The studies were carried out using an Everhart-Thornley secondary electron detector with extra high

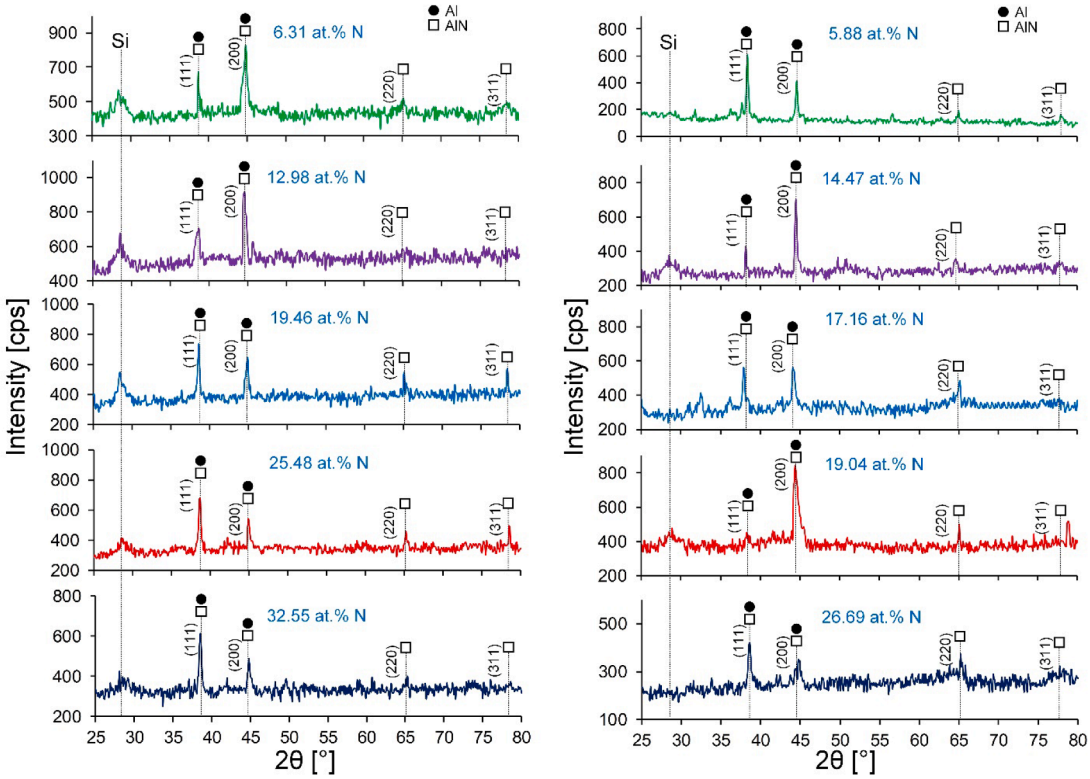

Fig.1. XRD measurements for the coatings under study.

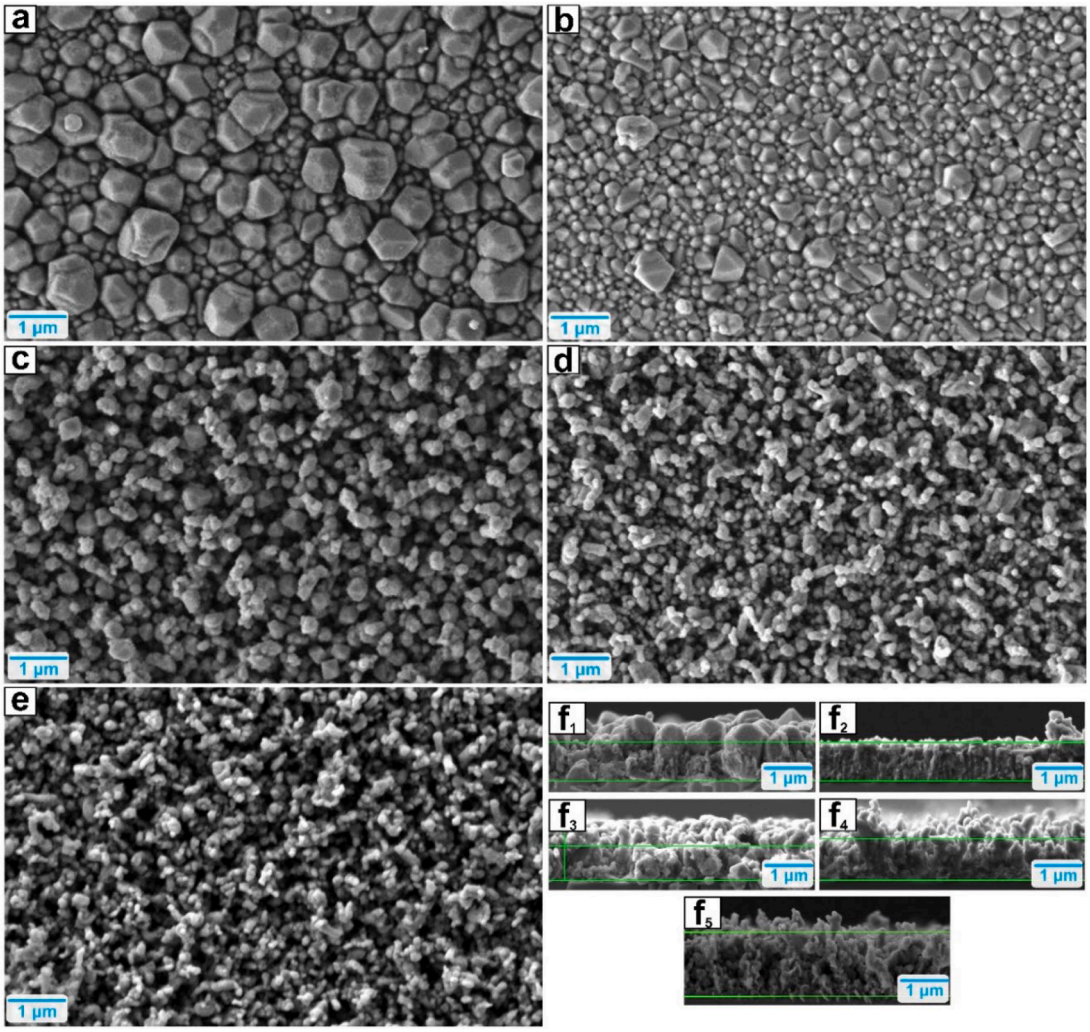

Fig. 2. SEM images of the surface (a-e) and cross sections (f_1-f_5) of coatings of group 1: a – $Al_{0.94}N_{0.06}$; b – $Al_{0.87}N_{0.13}$; c – $Al_{0.81}N_{0.19}$; d – $Al_{0.75}N_{0.25}$; e – $Al_{0.67}N_{0.33}$; f_1 – $Al_{0.94}N_{0.06}$; f_2 – $Al_{0.87}N_{0.13}$; f_3 – $Al_{0.81}N_{0.19}$; f_4 – $Al_{0.75}N_{0.25}$; f_5 – $Al_{0.67}N_{0.33}$.

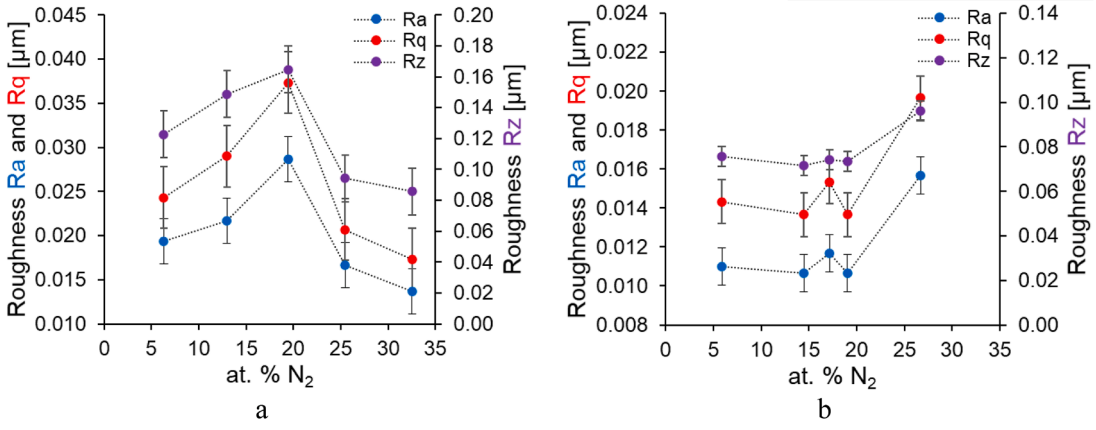

Fig. 3. Surface roughness: a – group 1; b – group 2.

tension (EHT) of 3 kV. After this, the samples were glued to the positioning table using conductive tape and the microstructure of their surface was studied, the EHT was 3 kV as well. Additionally, the microstructure of the coatings was assessed using Dimension FastScan (Bruker, USA) atomic force microscope (AFM) in the PeakForce QNM (Quantitative Nanoscale Mechanical Mapping) mode. The standard CSG10_SS silicon cantilevers (TipsNano, Russia) with a cantilever stiffness of 0.3 N/m and a tip radius of 10 nm were used.

The X-ray structural studies of coatings were carried out on an automated complex based on a DRON-3 M diffractometer (Burevestnik, Russia) in CuKα radiation using secondary monochromatization of the X-ray beam during step-by-step (0.1°) shooting with a pulse set duration

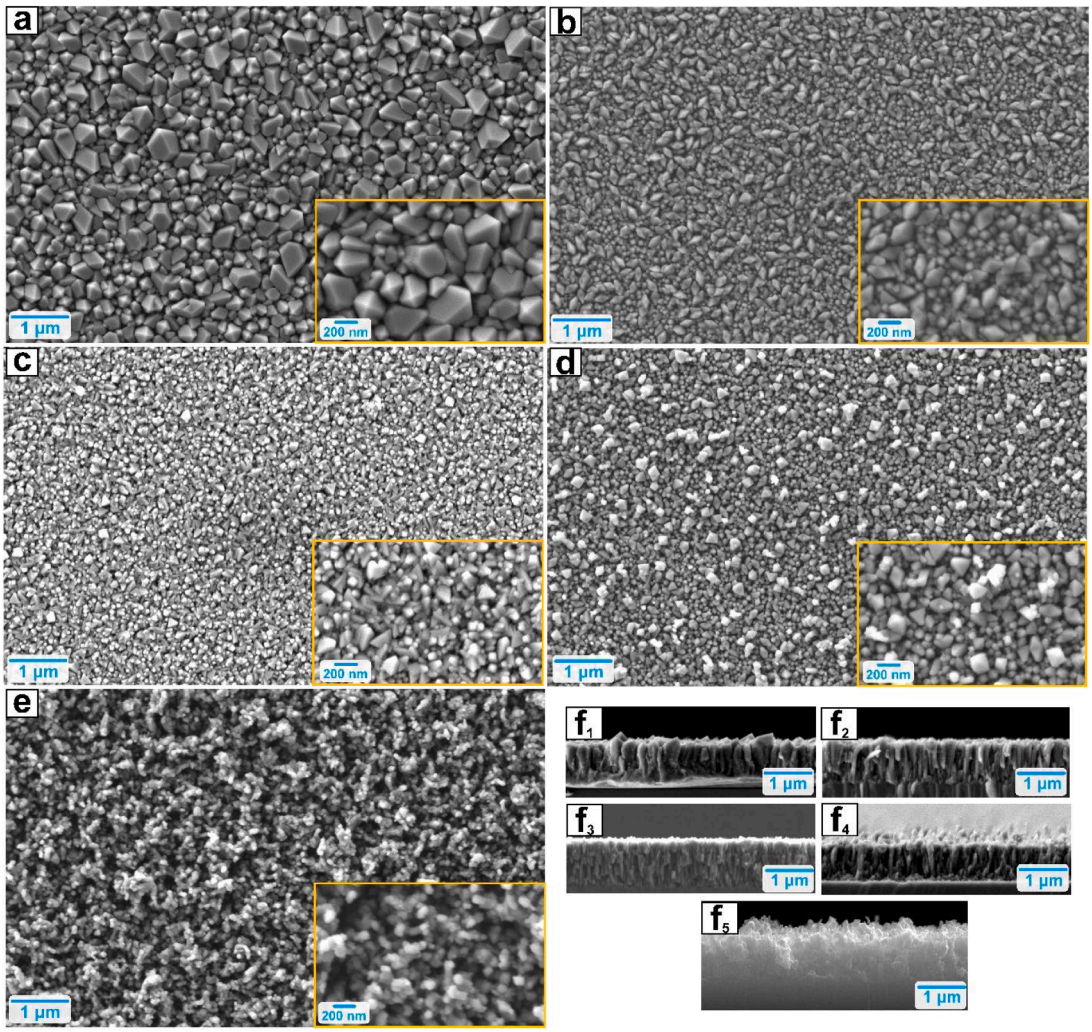

Fig. 4. SEM images of the surface (a-e) and cross sections (f_1-f_5) of coatings of group 2: a – $Al_{0.94}N_{0.06}$; b – $Al_{0.86}N_{0.14}$; c – $Al_{0.81}N_{0.19}$; d – $Al_{0.83}N_{0.17}$; e – $Al_{0.73}N_{0.27}$; f_1 – $Al_{0.94}N_{0.06}$; f_2 – $Al_{0.86}N_{0.14}$; f_3 – $Al_{0.81}N_{0.19}$; f_4 – $Al_{0.83}N_{0.17}$; f_5 – $Al_{0.73}N_{0.27}$.

at each point of 20 s.

The surface roughness of the coatings was determined using Surftest SJ-210 contact profilometer (Mitutoyo, Japan). Three profiles of 2.5 mm long were evaluated on each coating to determine roughness parameters (R_a, R_q, R_z). Roughness parameters were also obtained using AFM.

The stoichiometric composition and chemical analysis of the coatings were assessed using an EDX Oxford X-Max 80 (Oxford Instruments, UK) with 200x magnification and a voltage of 20 kV, from the sample surface over the entire area with a wide coverage (approximately ~150–200 μm by ~400–500 μm), as well as from individual contrast crystals pointwise.

The mechanical properties were determined using a Hysitron 750Ubi (Bruker, USA) nanoindentation system. A diamond conical indenter with a radius of curvature of 226 nm and an angle of 60° at the apex was used. The mechanical properties were determined at a maximum load of 100 μN, the results were averaged for 9 indentations for each sample. The indentation depth did not exceed the 1/10 of the coating thickness. The microtribological properties were determined using the same device and indenter. To conduct microtribological tests (nanoscratch testing), the nanoindenter was equipped with a two-dimensional transducer. Tests were carried out using specified functions of load and scratch length. During testing, 3 scratches 6 μm long were applied to each sample in 15 s with a constant load of 50, 75 and 100 μN – for AlN coatings. Multi-cycle tests consisted of applying 3 scratches of 6 μm length in 10 cycles of 5 s/cycle (total path 60 μm, duration 50 s) at a load of 100 μN for AlN coatings. The process of applying 3 scratches with a length of 5 μm in 100 cycles of 5 s/cycle (total path 500 μm, duration 500 s) was carried out with a load of 100 μN for all samples. Scratching of the surface with an increasing load up to 1000 μN was carried out for AlN coatings over a distance of 5 μm in 5 ss. The specific volumetric wear (ω) after 100 cycles was calculated from the volume of material removed during the friction test divided by the product of load and distance.

The specific surface electrical resistivity ρ was determined according to formula:

$$R_{\square} = \frac{\rho}{d},$$

where d – is coating thickness, m; $R_{\square}$ – surface resistance [Ω/□] (Ohm per square). Surface resistance $R_{\square}$ was measured using the four-probe method on the IUS-3 (SamaraPribor, Russia) unit.

3. Results and discussion

According to the EDX results, the atomic content of nitrogen in the coating composition increases, and aluminum decreases (Table 2). The change in Al and N in coatings depends almost linearly on the nitrogen flow in the chamber during coating deposition.

In the diffraction patterns of the deposited AlN coatings, diffraction lines emanating from the AlN cubic phase were observed (Fig. 1). At nitrogen concentrations of 6.31 and 5.88 at.% N ($Al_{0.94}N_{0.06}$ and

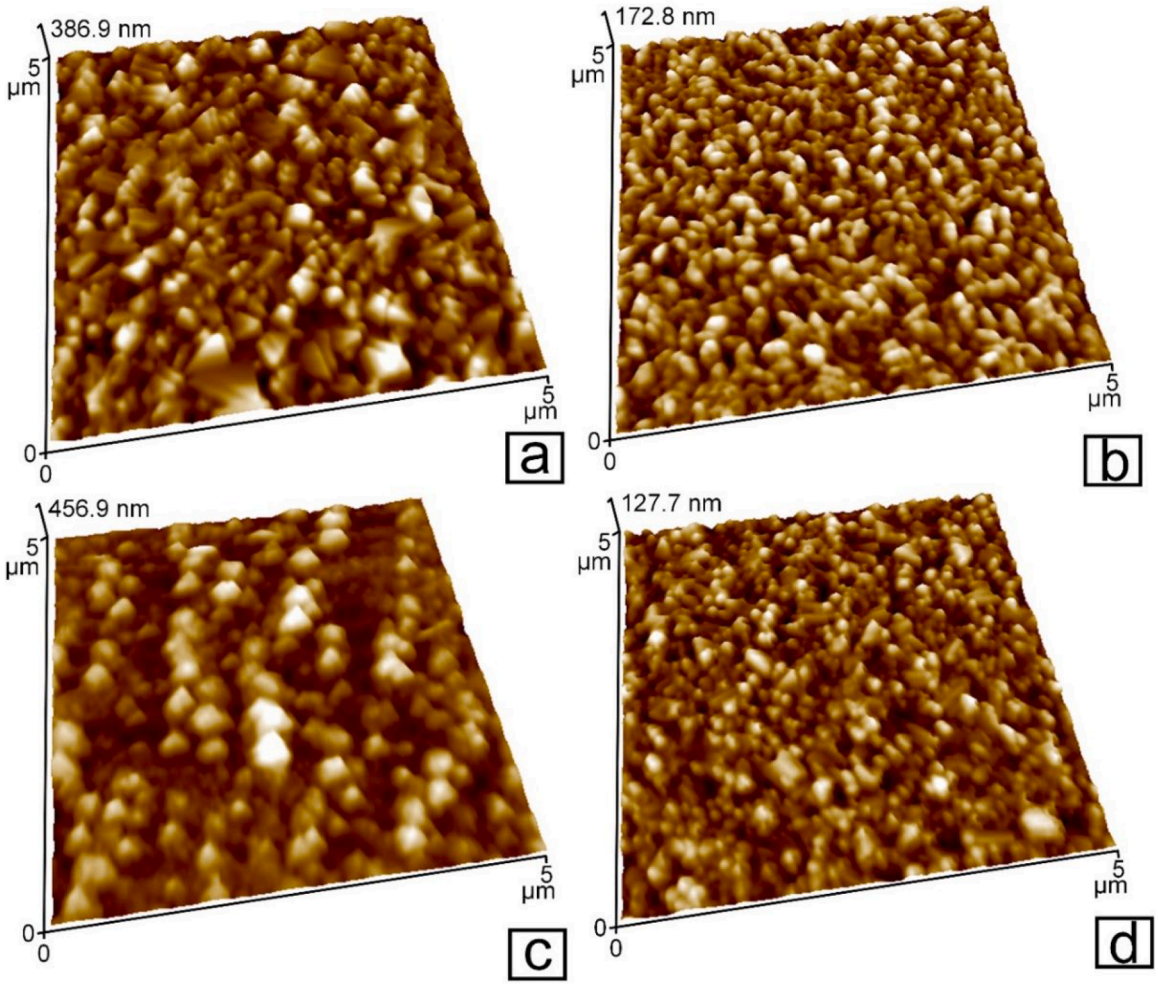

Fig. 5. AFM images of the surface (a-d) of coatings of group 2: a – $Al_{0.94}N_{0.06}$; b – $Al_{0.86}N_{0.14}$; c – $Al_{0.81}N_{0.19}$; d – $Al_{0.83}N_{0.17}$.

$Al_{0.94}N_{0.06}$), the presence of the Al phase together with the AlN phase of (111), (200), (220) and (311) orientations was observed in the coatings (Fig. 1). The main peaks in all coatings representing the cubic crystal structure are the (111) and (200) peaks.

SEM and AFM studies demonstrated differences in microstructure and surface roughness between the samples with AlN coatings (Figs. 2–5). The structure of the $Al_{0.94}N_{0.06}$ and $Al_{0.87}N_{0.13}$ coatings in the first group consists of multifaceted crystallites of various sizes. Their size decreases with increasing nitrogen content from 6.31 to 12.98 at.% N ($Al_{0.94}N_{0.06}$ and $Al_{0.87}N_{0.13}$ coatings, Fig. 2a,b). Crystallites with a size of 0.7–1.0 μm predominate on the surface of the $Al_{0.94}N_{0.06}$ coating. On the $Al_{0.87}N_{0.13}$ coating, their number decreases significantly and crystallites with a size of 50–250 nm are uniformly distributed over the entire surface.

A further increase in nitrogen content to 19.46–32.55 at.% N leads to a change in the surface structure from crystallite to granular (Fig. 2c–e). On the surface of the $Al_{0.81}N_{0.19}$ coating (Fig. 2c) there is an insignificant amount of crystallites similarly to $Al_{0.87}N_{0.13}$ coating (Fig. 2b), and on the $Al_{0.75}N_{0.25}$ and $Al_{0.67}N_{0.33}$ coatings (with 25.48 and 32.55 at.% N) they are absent. The surface structure of coatings of group 1 also changes from crystallite to granular, the corresponding changes in their microgeometrical characteristics are shown in Fig. 3a. When the nitrogen content changes from 6.31 to 19.46 at.% N, the roughness increases, and then decreases as the nitrogen content increases from 19.46 to 32.55 at. % N.

The structure of the second group of samples (Fig. 4) also changes with increasing nitrogen content. The $Al_{0.94}N_{0.06}$ coating (Figs. 4a, 5a) is almost similar in structure to the $Al_{0.87}N_{0.13}$ coating (Fig. 2b) in the first group. The structure is represented by crystallites with a size of 500 nm or less. On the surface of the $Al_{0.86}N_{0.14}$ coating there are crystallites of elongated rhomboid shape (Figs. 4b, 5b) with sizes from 20 to 300 nm. A similar structure, consisting of diamond-shaped crystallites, was obtained in [16] during AlN coating deposition by varying the ratio of argon and nitrogen concentrations in the chamber.

With an increase in nitrogen content to 17.16 and 19.04 at.% N, the structure changes to fine-grained with an insignificant presence of crystallites of multifaceted, rhomboid and triangular shapes (Figs. 4c,d, 5c,d). The grain size is 10–30 nm, and the crystallites are 50–200 nm. The surface structure of the $Al_{0.73}N_{0.27}$ coating (Fig. 4e) is similar to the structure of the $Al_{0.75}N_{0.25}$ and $Al_{0.67}N_{0.33}$ coatings of the first group (Fig. 2d,e), but has a smaller grain size (Fig. 4e). The surface roughness of coatings of group 1 also changes from crystallite to granular A similar granular structure of the coating surface was obtained in [22] at a deposition pressure of 0.2–0.55 Pa and with increasing pressure the grain size decreased.

It should be noted that on the surface of crystallites on the $Al_{0.94}N_{0.06}$ and $Al_{0.87}N_{0.13}$ coatings (Fig. 2a,b) in the first group and $Al_{0.94}N_{0.06}$ and $Al_{0.86}N_{0.14}$ coatings in the second group (Fig. 4a,b) the regular planes in the form of a triangle, square, rhombus and polygon were observed. According to [16] this type of crystallites are single crystals.

The cross section of each sample of group 1 (Fig. 2f_1-f_5) shows that $Al_{0.94}N_{0.06}$ and $Al_{0.87}N_{0.13}$ coatings are formed in the form of a columnar structure oriented perpendicular to the substrate (Fig. 2f_1 and f_2), and $Al_{0.81}N_{0.19}$, $Al_{0.75}N_{0.25}$ and $Al_{0.67}N_{0.33}$ coatings – in the form of dendritic

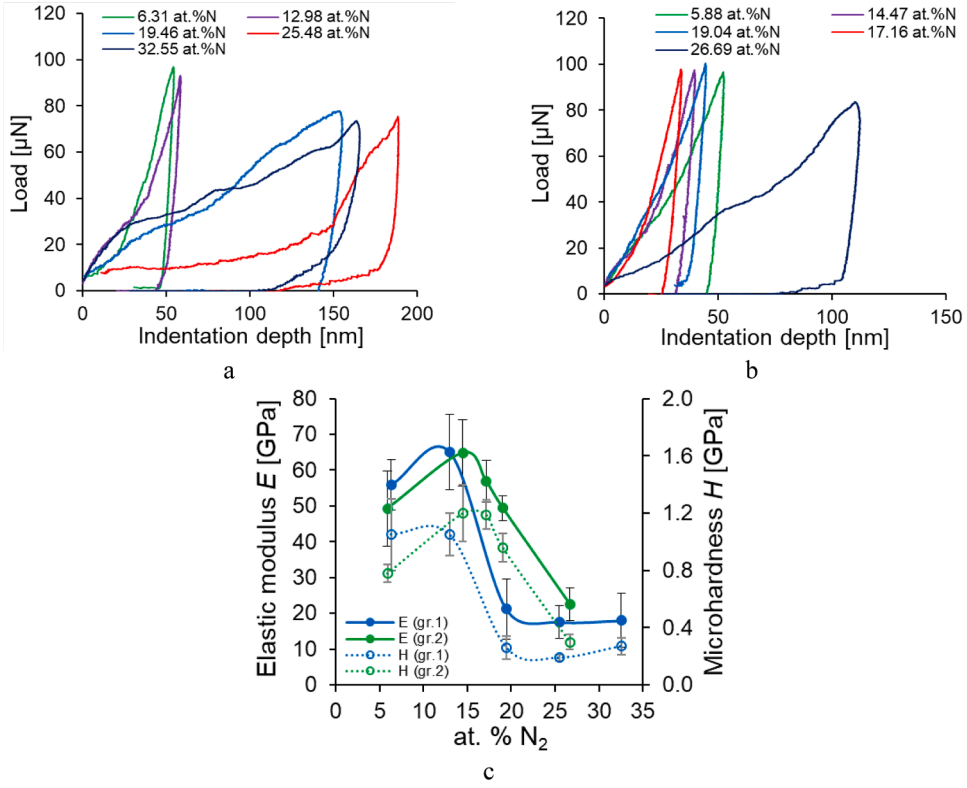

Fig. 6. Indentation curves for the group 1 (a) and group 2 (b) and mechanical properties (c) of AlN coatings.

structure (Fig. 2f_3-f_5). The columnar structure of AlN coating formation was also obtained in [20]. The columnar structure is very similar to the band model of magnetron sputtered coatings described in [20] and proposed in [28]. In this case, the change in the size of the columns on the cross section in the model depends on the change in the deposition parameters (power, temperature and time deposition) [20,28]

Coatings of group 2 (except for the $Al_{0.73}N_{0.27}$ coating) are formed in the form of a columnar structure (Fig. 3f_1-f_4). The $Al_{0.73}N_{0.27}$ coating (Fig. 3f_5) is similar in structure to $Al_{0.81}N_{0.19}$, $Al_{0.75}N_{0.25}$ and $Al_{0.67}N_{0.33}$ coatings of group 1 – it demonstrates a dendritic structure.

The thickness of the coatings was determined from the cross section (Fig. 2f_1-f_5, Fig. 4f_1-f_5). The results obtained demonstrate that the thickness does not depend on the nitrogen flow in the chamber during deposition for the samples under study (Table 2). It varies in the range from 725 to 1220 nm (Table 2, Fig.s 2f_1-f_5 and 4f_1-f_5).

When comparing changes in the chemical composition and images of the structure, it can be noted that when 15–20 at.% nitrogen in the coating composition is exceeded, the crystalline structure changes to granular and the columnar transverse structure to dendritic for both groups of AlN coatings.

The mechanical properties of the coatings increase with increasing the nitrogen content up to 15 at.% N (Fig. 6). For group 1 AlN coatings, the elastic modulus E increases from 56±7 GPa to 65±11 GPa, and the microhardness H remains constant and is equal to 1.1 ± 0.3 GPa. For the second group of coatings, E increases to 65±11 GPa, and microhardness – to 1.2 ± 0.2 GPa. The values of microhardness and elastic modulus obtained at such nitrogen concentrations are close in value to aluminum coatings [17,21], deposited by the magnetron method onto a silicon substrate at a higher power compared to the power used in this work (750 W).

When the nitrogen content increases to 20 at.% N, there is a sharp decrease in E and H in the first group of coatings – to 21±8 GPa and 0.3 ± 0.1 GPa, respectively. In the second group, a concentration of 17–20 at.% N leads to a slight decrease in the elastic modulus to 49±3 GPa. In this case, the microhardness remains almost constant – 1.2 ± 0.1 GPa. A further increase in the nitrogen concentration in the coatings reduces the elastic modulus and microhardness in two groups of coatings. In the first group at the $Al_{0.67}N_{0.33}$ coating $E = 18±8$ GPa and $H = 0.3 \pm 0.1$ GPa, in the second one at the $Al_{0.73}N_{0.27}$ coating 26.69 at.% N $E = 23±5$ GPa and $H = 0.3 \pm 0.1$ GPa.

Both in the microstructure and in the mechanical properties, there is a sharp change in properties when the nitrogen concentration in the coatings changes in the range from 15 to 20 at.% N. The mechanical properties in this work are lower compared to other sources [16,29,30]. However, it should be noted that other sources discuss coatings with a higher nitrogen content in the coating composition (>40 at.% N). Thus, low microhardness was obtained in AlN coatings with 28 at.% N, described in [29] and amounted to 2 GPa.

Changes in microstructure and mechanical properties are associated with changes in the crystal structure of coatings [29,30]. In the first group, changing the ratio of the intensities of the (111) and (200) peaks (Fig. 1) lead to a change in the microstructure of the structure from crystallite to granular (Fig. 2) one, as well as a change in the mechanical properties (Fig. 6c). The constant change in the predominant phase orientation of cubic AlN in the second group also leads to a change in the microstructure (Fig. 4) and mechanical properties (Fig. 6c).

The coefficient of friction CoF in microtests for group 1 decreases to 0.196–0.284 at three constant loads (50, 75 and 100 μN) with an increase from 6.31 to 12.98 at.% N in the coating composition (Fig. 7a). A similar decrease occurs in the second group of coatings – to 0.150–0.185. This is explained by an increase in the mechanical properties of the coatings in this range of at.% N (Fig. 6). Similar CoF values (after tribotests on a microtribometer using a ball-disk scheme with a steel ball with a diameter of 3 mm) were obtained in [17] and are in the range of 0.143–0.447 depending on the thickness of the AlN layers in multilayer Al/AlN coatings, and in a single-layer CoF coating friction was 0.324.

The coefficient of friction changes to maximum values of 1.031–1.191 on the $Al_{0.81}N_{0.19}$ coating from the first group of samples. In this case, the influence of roughness occurs (Fig. 3a, at this

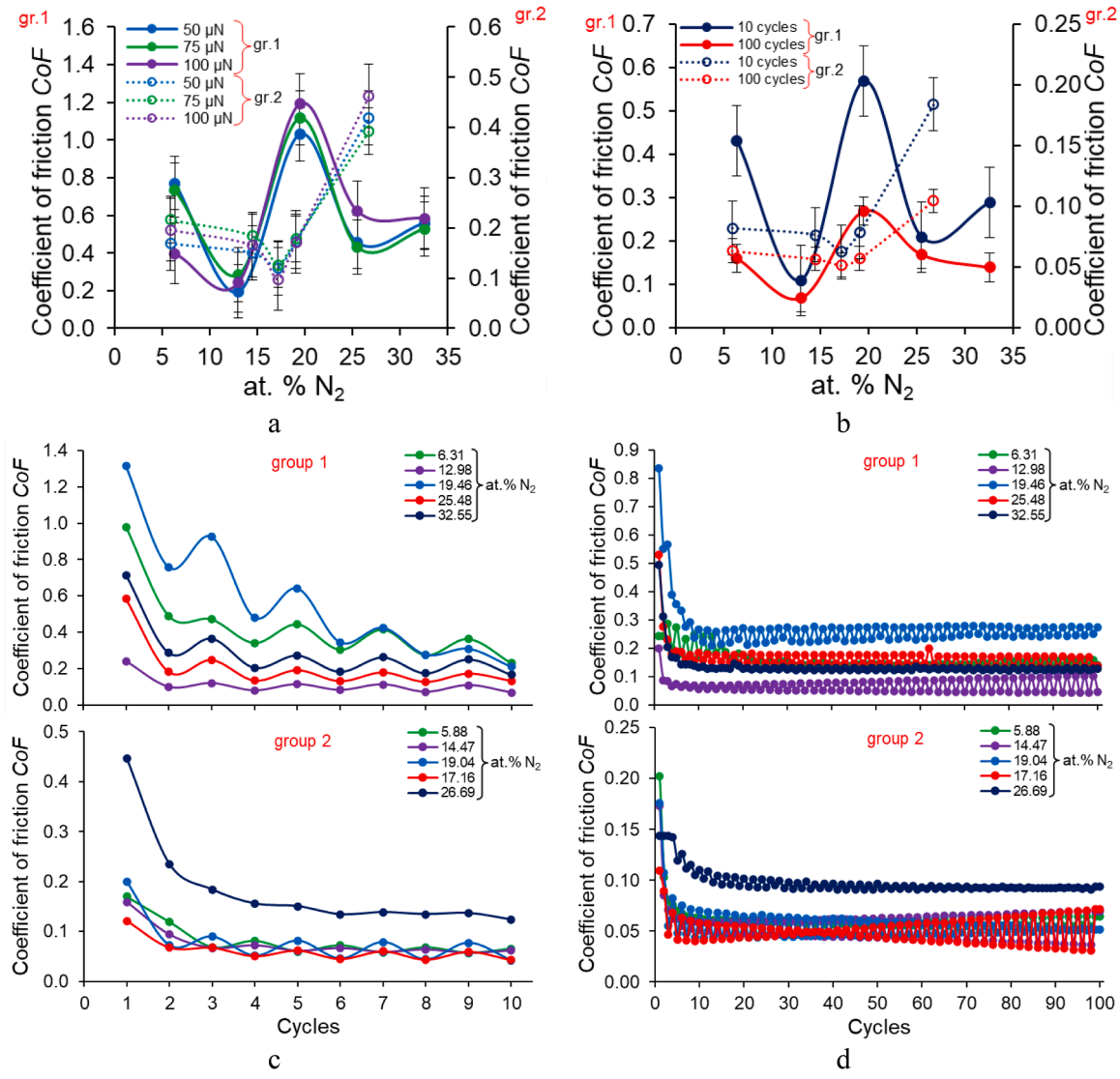

Fig. 7. Tribological properties of AlN coatings for groups 1 and 2: a – CoF at constant load (50, 75 and 100 μN); b – CoF after 10 and 100 cycles; c, d – dependence of CoF on the number of cycles.

Table 3
C_{corr} of roughness with coefficient of friction under various test conditions and specific volumetric wear.

		CoF					***ω***
		10 cycles	100 cycles	50 μN	75 μN	100 μN	(after 100 cycles)
Ra	group	0.6	0.6	0.5	0.7	0.6	−0.3
Rq	1	0.5	0.5	0.5	0.6	0.5	−0.3
Rz		0.4	0.3	0.3	0.5	0.3	−0.5
Ra	group	1.0	0.9	0.9	0.9	0.9	0.9
Rq	2	0.9	0.9	0.9	0.9	0.9	0.9
Rz		1.0	1.0	1.0	1.0	1.0	1.0

concentration it increases). The increase in the coefficient of friction is also associated with a decrease in the mechanical properties of this coating (Fig. 6). In group 2, CoF decreases on the $Al_{0.83}N_{0.17}$ coating, and then CoF increases with increasing at.% N (Fig. 7a,b).

In this work, high-cycle friction tests allowed to study the behavior of coatings in microcontact. As a result of multi-cycle friction, an identical change in the coefficient of friction was demonstrated after 10 and 100 friction cycles (Fig. 7b). Higher values of the coefficient of friction after 10 cycles (Fig. 7c) can be explained by the fact that the diamond conical indenter tends to interact to a greater extent with all surface irregularities during the first cycles and it requires more effort to overcome them. And the higher they are, the greater is the coefficient of friction. Then, with each cycle, these irregularities are smoothed out and the interaction is reduced, which leads to a decrease in the CoF values. Also, it should be noted that during microfriction in the contact area of the indenter tip with the surface, high stresses arise, several times higher than the contact stresses during standard tribotesting, and amount to tens of GPa [31,32], which leads to faster wear of the surface. In the range of cycles from 10 to 100, the coefficient of friction remains almost stable for each coating and varies within a standard deviation around the average value.

Based on the results of microtribotests, it was established that the CoF (for all types of tests) completely correlates with the roughness in group 2 (Table 3) – the correlation coefficient is 0.9–1.0 (high direct correlation). For group 1, the CoF values of group 1 practically do not correlate with roughness (Table 3).

Microscratch testing with increasing load showed that the most stable coating in group 1 was the $Al_{0.87}N_{0.13}$ coating (Fig. 8a, purple diagram). On this coating, the minimum CoF values were also obtained in other tests – 0.068 (after 100 test cycles), 0.109 (after 10 test cycles),

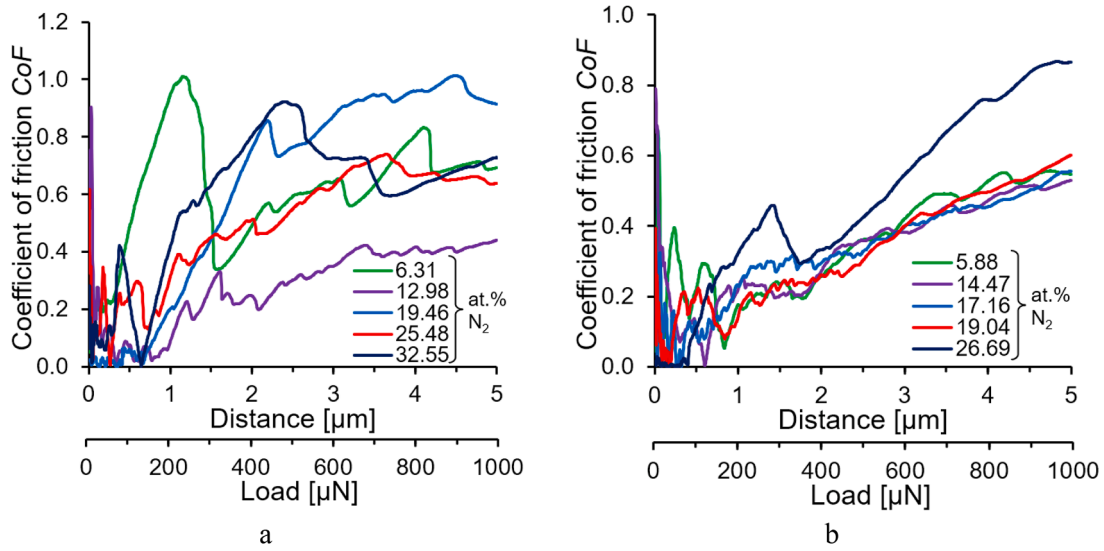

Fig. 8. Tribological properties of AlN coatings for groups 1 (a) and 2 (b) with increasing load from 0 to 1000 μN.

Table 4
Correlation coefficients of stoichiometric composition with the properties of AlN coatings.

	E	*H*	*CoF*					*ω*
			10 cycles	100 cycles	50 μN	75 μN	100 μN	(after 100 cycles)
at. % N (gr.1)	**−0.8**	**−0.9**	−0.2	0.1	−0.1	−0.1	0.3	**0.8**
at. % N (gr.2)	−0.6	−0.5	**0.7**	0.6	**0.7**	0.6	0.6	0.6

0.196 (at a load of 50 μN), 0.284 (at a load of 75 μN), 0.244 (at a load of 100 μN). All other coatings demonstrate a higher CoF and there is a large difference in values (Fig. 8a). The coatings in group 2 showed almost identical CoF diagrams with increasing load (Fig. 8b). Only the $Al_{0.73}N_{0.27}$ coating turned out to be less resistant to such tests (Fig. 8b, dark blue line) – with large differences in the CoF values in the diagram.

When determining the correlation of physical, mechanical and microtribological properties with the stoichiometric composition, it was established (Table 4) that the composition of group 1 is more correlated with the elastic modulus and microhardness of coatings, and the composition of group 2 is more correlated with the coefficient of friction and specific volumetric wear.

Specific volumetric wear *ω* (Fig. 9) as well as the coefficient of friction in the second group depends on the surface roughness – correlation coefficient 0.9–1.0 (high direct correlation) (Table 3), but does not depend on the composition of the coatings (Table 4). Fig. 9 shows images of the wear area after 100 cycles. The greatest wear depth of 265 nm was obtained on a $Al_{0.81}N_{0.19}$ coating of the first group, and in the second group – 189 nm on a $Al_{0.73}N_{0.27}$ coating (Fig. 9a). For both groups of coatings, specific volumetric wear decreases with increasing nitrogen content to 15–20 at %. In group 1, specific volumetric wear decreases from 0.68 ± 0.03 m^3/N·m for $Al_{0.94}N_{0.06}$ coating to 0.38 ± 0.02 m^3/N·m for $Al_{0.87}N_{0.13}$ coating, and in group 2 – from 0.42 ± 0.02 m^3/N·m for $Al_{0.94}N_{0.06}$ coating to 0.12 ± 0.01 m^3/N·m for $Al_{0.83}N_{0.17}$ coating. An increase in specific volumetric wear was observed as well: in the first group this is associated with a decrease in physical and mechanical properties (Fig. 6), in the second group – with an increase in surface roughness (Fig. 3). The maximum values of ω were obtained for the $Al_{0.75}N_{0.25}$ coating (ω = 1.76 ± 0.09 m^3/N·m) of the first group, and in the second group for the $Al_{0.73}N_{0.27}$ coating (ω = 1.07 ± 0.05 m^3/N·m).

Based on the results of measuring the specific electrical resistivity of the coating surface using the four-probe method, it was established that with increasing at % N, the value of ρ increases (Fig. 10), i.e. the conductivity of the coating decreases. It should be noted that at concentrations up to 15 – 20 at % N resistivity increases more slowly than at high nitrogen concentrations in coatings – its dependence on the composition of the coating, as well as microstructure, mechanical and tribological properties was found. The minimum values were obtained as 0.098 and 0.133 μΩ·m for coatings with 6.31 (gr.1, $Al_{0.94}N_{0.06}$) and 5.88 (gr.2, $Al_{0.94}N_{0.06}$) at.% N, respectively. Coatings with the best mechanical and microtribological characteristics ($Al_{0.87}N_{0.13}$ coating in the first group and $Al_{0.83}N_{0.17}$ coating in the second group) have electrical resistivity of 0.168 and 0.918 μΩ·m, respectively.

When determining the correlation of the electrical resistivity of coatings with the stoichiometric composition, thickness and physical and mechanical properties, it was found that group 1 of AlN coatings depends on the thickness of the coating (C_{corr} = 0.9) and nitrogen content (C_{corr} = 0.9), and the second group AlN depends on the nitrogen content (C_{corr} = 0.9) and correlates with the elastic modulus of the coatings (C_{corr} = −0.8).

4. Conclusions

As a result of this work, two groups (the first group of coatings was sputtered at 100 °C, the second one – at 20 °C) of AlN coatings with different stoichiometric compositions were obtained using the reactive DC magnetron sputtering method with the variable nitrogen flow in the chamber. According to the results of X-ray phase analysis, the deposited AlN coatings are represented by the AlN cubic phase. The structure of the coatings of both groups with a nitrogen content of up to 15–20 at.% N consists of single crystals – crystallites with regular planes. With a further increase in at.% N, the structure changes to granular. Both in the microstructure and in the mechanical properties a sharp change in properties when the nitrogen concentration in the coatings varied in the range from 15 to 20 at.% N was observed.

The CoF for coatings of group 1 decreases to 0.196–0.284 with an increase from nitrogen concentration 6.31 to 12.98 at.% N, and in group

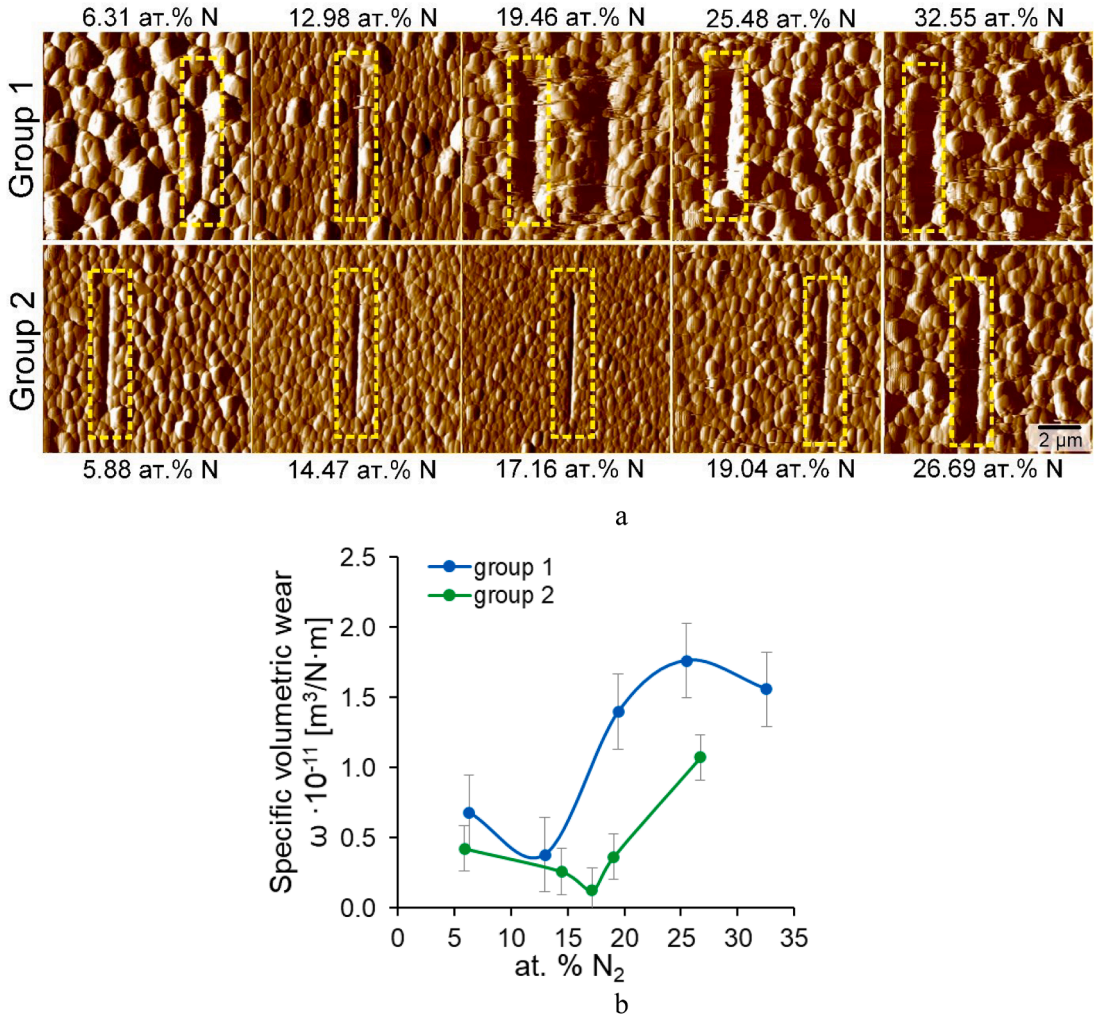

Fig. 9. AFM images of the wear area after 100 microfriction cycles (a) and specific volumetric wear after 100 cycles obtained during tribological tests.

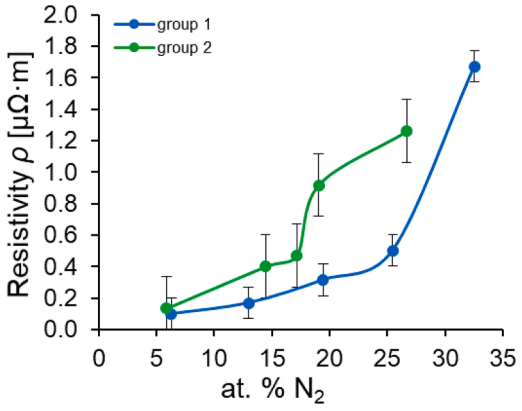

Fig. 10. Electrical resistivity of AlN coatings.

2 it decreases to 0.150–0.185 with an increase from 5.88 to 17.16 at.% N, which is associated with an increase in the mechanical properties of the coatings. With a further increase in nitrogen concentration, CoF increases due to an increase in the roughness of the coatings and a decrease in mechanical properties. Specific volumetric wear of the AlN coatings depends the mechanical properties and surface roughness. The specific electrical resistivity of the coatings surfaces increases with increasing nitrogen concentration. Thus, from the point of view of the optimal combination of microstructure, mechanical, tribological properties, as well as relatively low specific electrical resistivity, the most preferred coatings are: in group 1 – $Al_{0.87}N_{0.13}$ coating, in group 2 – $Al_{0.83}N_{0.17}$ coating.

CRediT authorship contribution statement

Vasilina Lapitskaya: Writing – review & editing, Writing – original draft, Visualization, Validation, Software, Project administration, Methodology, Investigation, Funding acquisition, Formal analysis, Data curation, Conceptualization. **Andrey Nikolaev:** Writing – review & editing, Resources, Methodology, Investigation, Formal analysis, Data curation, Conceptualization. **Anastasiya Khabarava:** Investigation, Formal analysis. **Evgeniy Sadyrin:** Writing – review & editing, Methodology, Investigation, Formal analysis. **Sergei Aizikovich:** Supervision, Resources, Project administration, Methodology, Funding acquisition, Conceptualization. **Aleksandr Komarov:** Investigation, Formal analysis. **Dmitry Orda:** Investigation, Formal analysis. **Aleksandra Cherniavskaya:** Investigation, Formal analysis. **Kamaludin Abdulvakhidov:** Investigation, Formal analysis. **Anaid Azoyan:** Investigation, Formal analysis. **Dmitry Kotov:** Investigation, Formal analysis. **Sergei Chizhik:** Supervision, Resources, Project administration, Methodology, Data curation, Conceptualization.

Declaration of competing interest

The authors declare that they have no known competing financial interests or personal relationships that could have appeared to influence the work reported in this paper.

Acknowledgment

Lapitskaya V., Khabarava A. and Chizhik S. acknowledges the support of the Belarus Republican Foundation for Fundamental Research (grant No T23RNF-132), Nikolaev A. acknowledges the support of the Russian Science Foundation (grant No 23–49–10062, https://rscf.ru/project/23-49-10062/).

Data availability

The authors do not have permission to share data.

References

[1] A.F. Belyanin, L.L. Bouilov, V.V. Zhirnov, A.I. Kamenev, K.A. Kovalskij, B. V. Spitsyn, Application of aluminum nitride films for electronic devices, Diam. Relat. Mater. 8 (1999) 369–372, https://doi.org/10.1016/s0925-9635(98)00412-9.

[2] M.A. Moreira, I. Doi, J.F. Souza, J.A. Diniz, Electrical characterization and morphological properties of AlN films prepared by dc reactive magnetron sputtering, Microelectron. Eng. 88 (2011) 802–806, https://doi.org/10.1016/j.mee.2010.06.045.

[3] Q.S. Paduano, D.W. Weyburne, J. Jasinski, Z. Liliental-Weber, Effect of initial process conditions on the structural properties of AlN films, J. Cryst. Growth 261 (2004) 259–265, https://doi.org/10.1016/j.jcrysgro.2003.11.017.

[4] J. Du, W. Dai, H. Kou, P. Wu, W. Xing, Y. Zhang, C. Zhang, AlN coatings with high thermal conductivity and excellent electrical properties for thermal management devices, Ceram. Int. 49 (2023) 16740–16752, https://doi.org/10.1016/j.ceramint.2023.02.035.

[5] H. Cheng, Y. Sun, J.X. Zhang, Y.B. Zhang, S. Yuan, P. Hing, AlN films deposited under various nitrogen concentrations by RF reactive sputtering, J. Cryst. Growth 254 (2003) 46–54, https://doi.org/10.1016/S0022-0248(03)01176-X.

[6] V. Moraes, H. Riedl, R. Rachbauer, S. Kolozsvári, M. Ikeda, L. Prochaska, S. Paschen, P.H. Mayrhofer, Thermal conductivity and mechanical properties of AlN-based thin films, J. Appl. Phys. (2016) 119, https://doi.org/10.1063/1.4953358.

[7] M. Khan, G.A. Nowsherwan, A.A. Shah, S. Riaz, M. Riaz, A.D. Chandio, A.K. Shah, I.A. Channa, S.S. Hussain, R. Ali, et al., A study of the structural and surface morphology and photoluminescence of Ni-doped AlN thin films grown by Co-sputtering, Nanomater 12 (2022) 3919, https://doi.org/10.3390/NANO12213919.

[8] R. Ding, W. Xuan, S. Dong, B. Zhang, F. Gao, G. Liu, Z. Zhang, H. Jin, J. Luo, The 3.4 GHz BAW RF filter based on single crystal AlN resonator for 5G application, Nanomater 12 (2022) 3082, https://doi.org/10.3390/NANO12173082.

[9] V.R. Shayapov, A.L. Bogoslovtseva, S.Y. Chepkasov, I.P. Asanov, E. A. Maksimovskiy, A.V. Kapishnikov, M.I. Mironova, A.V. Lapega, P.V. Geydt, Chemical composition, structure, and physical properties of AlN films produced via pulsed DC reactive magnetron sputtering, Coatings 13 (2023) 1281, https://doi.org/10.3390/COATINGS13071281/S1.

[10] M.A. Auger, L. Vázquez, M. Jergel, O. Sánchez, J.M. Albella, Structure and morphology evolution of ALN films grown by DC sputtering, Surf. Coat. Technol. 180–181 (2004) 140–144, https://doi.org/10.1016/j.surfcoat.2003.10.054.

[11] H.P. Loebl, M. Klee, C. Metzmacher, W. Brand, R. Milsom, P. Lok, Piezoelectric thin AlN films for bulk acoustic wave (BAW) resonators, Mater. Chem. Phys. 79 (2003) 143–146, https://doi.org/10.1016/S0254-0584(02)00252-3.

[12] L.M. Petrov, K.V. Grigorovich, G.S. Sprygin, S.B. Ivanchuk, A.N. Smirnova, V. D. Semenov, Formation of transition gradient layers in the process of creating a surface composite “steel-coating (Al, Al-N)” at VIP treatment, J. Phys. Conf. Ser. (2019) 1281, https://doi.org/10.1088/1742-6596/1281/1/012060.

[13] M. Nakamura, S. Kubota, H. Suzuki, T. Haraguchi, Wear and friction characteristics of AlN/diamond-like carbon hybrid coatings on aluminum alloy, J. Mater. Eng. Perform. 24 (2015) 3789–3797, https://doi.org/10.1007/s11665-015-1694-8.

[14] Z. Zhang, Z. Chen, D. Holec, C.H. Liebscher, N. Koutná, M. Bartosik, Y. Zheng, G. Dehm, P.H. Mayrhofer, Mapping the mechanical properties in nitride coatings at the nanometer scale, Acta Mater 194 (2020) 343–353, https://doi.org/10.1016/j.actamat.2020.04.024.

[15] M. Schlögl, B. Mayer, J. Paulitsch, P.H. Mayrhofer, Influence of CrN and AlN layer thicknesses on structure and mechanical properties of CrN/AlN superlattices, Thin Solid Films 545 (2013) 375–379, https://doi.org/10.1016/j.tsf.2013.07.026.

[16] J. Li, Y. Wang, L. Wang, Structure and protective effect of AlN/Al multilayered coatings on NdFeB by magnetron sputtering, Thin Solid Films 568 (2014) 87–93, https://doi.org/10.1016/j.tsf.2014.08.012.

[17] Z.G. Wu, G.A. Zhang, M.X. Wang, X.Y. Fan, P.X. Yan, T. Xu, Structure and mechanical properties of Al/AlN multilayer with different AlN layer thickness, Appl. Surf. Sci. 253 (2006) 2733–2738, https://doi.org/10.1016/j.apsusc.2006.05.039.

[18] C. Wang, W. Cheng, P. Ma, R. Xia, X. Ling, High performance Al-AlN solar spectrally selective coatings with a self-assembled nanostructure AlN anti-reflective layer, J. Mater. Chem. A 5 (2017) 2852–2860, https://doi.org/10.1039/c6ta09460k.

[19] D. Pan, J.K. Jian, A. Ablat, J. Li, Y.F. Sun, R. Wu, Structure and magnetic properties of Ni-doped AlN films, J. Appl. Phys. (2012) 112, https://doi.org/10.1063/1.4749408.

[20] C.C. Wang, C.J. Lu, M.H. Shiao, F.S. Shieu, Microstructural evolution of AlN coatings synthesized by unbalanced magnetron sputtering, J. Vac. Sci. Technol. A Vacuum, Surf., Film. 23 (2005) 621–627, https://doi.org/10.1116/1.1927532.

[21] X. Shi, S. Zhang, Y. You, D. Sun, X. Yu, J. Wang, H. Du, F. Li, Enhancing color tunability, corrosion resistance, and hardness of AlN/Al coatings on magnesium alloys via sputtering a Si interlayer, Vacuum 209 (2023) 111772, https://doi.org/10.1016/j.vacuum.2022.111772.

[22] Q.P. Wei, X.W. Zhang, D.Y. Liu, J. Li, K.C. Zhou, D. Zhang, Z.M. Yu, Effects of sputtering pressure on nanostructure and nanomechanical properties of AlN films prepared by RF reactive sputtering, Trans. Nonferrous Met. Soc. China (English Ed. 24 (2014) 2845–2855, https://doi.org/10.1016/S1003-6326(14)63417-8.

[23] M. Shahien, M. Yamada, T. Yasui, M. Fukumoto, In situ fabrication of AlN coating by reactive plasma spraying of Al/AlN powder, Coatings 1 (2011) 88–107, https://doi.org/10.3390/coatings1020088.

[24] C. Boulmer-Leborgne, A.L. Thomann, P. Andreazza, C. Andreazza-Vignolle, J. Hermann, V. Craciun, P. Echegut, D. Craciun, Excimer laser synthesis of thin AlN coatings, Appl. Surf. Sci. 125 (1998) 137–148, https://doi.org/10.1016/S0169-4332(97)00419-4.

[25] J.X. Zhang, H. Cheng, Y.Z. Chen, A. Uddin, S. Yuan, S.J. Geng, S. Zhang, Growth of AlN films on Si (100) and Si (111) substrates by reactive magnetron sputtering, Surf. Coat. Technol. 198 (2005) 68–73, https://doi.org/10.1016/j.surfcoat.2004.10.075.

[26] S. Liu, Y. Li, J. Tao, R. Tang, X. Zheng, Structural, surface, and optical properties of AlN thin films grown on different substrates by PEALD, Cryst 13 (2023) 910, https://doi.org/10.3390/CRYST13060910.

[27] A.L. Nikolaev, E.V. Sadyrin, I.O. Kharchevnikov, P.E. Antipov, V.A. Lapitskaya, A. S. Vasiliev, S.S. Volkov, Deposition and characterization of magnetron sputtered AlN coatings with variable stoichiometry, Altenbach, H., Eremeyev, V., in: Advances in Linear and Nonlinear Continuum and Structural Mechanics. Advanced Structured Materials, 198, Springer, Cham, 2023, pp. 357–367, https://doi.org/10.1007/978-3-031-43210-1_20, 2023

[28] R. Messier, A.P. Giri, R.A. Roy, Revised structure zone model for thin film physical structure, J. Vacuum Sci. Technol. A 2 (1984) 500, https://doi.org/10.1116/1.572604.

[29] Y. Zhang, J. Dai, G. Bai, H. Zhang, Microstructure and thermal conductivity of AlN coating on Cu substrate deposited by arc ion plating, Mater. Chem. Phys. 241 (2020) 122374, https://doi.org/10.1016/j.matchemphys.2019.122374.

[30] R.K. Choudhary, S.C. Mishra, P. Mishra, P.K. Limaye, K. Singh, Mechanical and tribological properties of crystalline aluminum nitride coatings deposited on stainless steel by magnetron sputtering, J. Nucl. Mater. 466 (2015) 69–79, https://doi.org/10.1016/j.jnucmat.2015.07.036.

[31] T. Kuznetsova, V. Lapitskaya, A. Khabarava, R. Trukhan, S. Chizhik, E. Torskaya, A. Mezrin, S. Fedorov, A. Rogachev, B. Warcholinski, Silicon addition as a way to control properties of tribofilms and friction of DLC coatings, Appl. Surf. Sci. 608 (2023) 155115, https://doi.org/10.1016/J.APSUSC.2022.155115.

[32] T. Kuznetsova, V. Lapitskaya, A. Khabarava, R. Trukhan, S. Chizhik, E. Torskaya, S. Fedorov, S. Aizikovich, E. Sadyrin, B. Warcholinski, Features of wear of DLC-Si coating under microcontact conditions during the formation of secondary structures, Compos. Struct. 316 (2023) 117039, https://doi.org/10.1016/J.COMPSTRUCT.2023.117039.